

# Correlations and non-local transport in a critical-gradient fluctuation model

J H Nicolau<sup>1</sup>, L García<sup>1</sup> and B A Carreras<sup>2</sup>

<sup>1</sup> Universidad Carlos III, 28911 Leganés, Madrid, Spain

<sup>2</sup> BACV Solutions, 110 Mohawk Road, Oak Ridge, Tennessee 37830, USA

E-mail: javherna@fis.uc3m.es

**Abstract.** A one-dimensional model based on critical-gradient fluctuation dynamics is used to study turbulent transport in magnetically confined plasmas. The model exhibits the self-organized criticality (SOC) dynamics. At the steady state, two regions are found: the outer one is close to critical state and the inner one remaining at the subcritical gradient. The gradient-flux relation exhibits a parabola-like profile centered in the most probable gradient following experimental studies. This is a signature of the non-locality of particle transport driven by avalanches: at the given position transport is due to gradients situated into closer but different positions. The R/S analysis, applied to the fluxes dynamics reveals memory and correlation. Different  $H$  exponents corresponding to different dynamical behavior are obtained. The flux at the edge exhibits long time correlations, which can be suppressed if the external drive or the system size is modified. On the other hand, we found that in the sub-critical region the quasiperiodicity is present in the avalanches.

## 1. Introduction

Since several decades transport in magnetically confined plasmas has been an important topic of research. Self Organized Criticality (SOC) dynamics has been introduced in the field of complex systems [1] and then used as a simple paradigm for turbulent transport studies in magnetically confined plasmas [2] [3]. The SOC systems have to be seen as a qualitative method for studying basic physical behavior. They exhibit some of the characteristics of the  $L$ -mode such as profile stiffness, Bohm scaling and superdiffusion [4], which are out of scope in the framework of the diffusive model.

Here we consider a one-dimensional transport model based on the critical-gradient fluctuations dynamics. This model was presented in Ref. [5]. It has the properties of a SOC system. However, the transport is represented by a continuous amount of particles instead of an integer amount. Within this approach, we make an analogy from the height  $h$  of a sandpile to the average particle density in the plasma.

In the present work we are studying some of the characteristics of this model as the non-diffusive transport, non-locality and long time correlations.

Recently, experimental data from different devices [6] indicated that the relation between gradient and radial flux is not linear as in a diffusive model. Our simple transport model exhibits the same behaviour. The gradient-flux relation is given by a parabola-like profile centered in the most probable gradient. This indicates the non-locality of avalanches as an underlying transport mechanism.



The long-time correlations have been observed in the model as expected in a SOC system. Through the R/S analysis [7] [8] the quasi-periodicities of the model, which were described in Ref. [9] are confirmed.

In addition, in magnetic nuclear fusion devices, the protection of the wall is an important issue. It must support high temperatures and heat pulses at long time scales. That is why the fluxes should be studied as global events rather than an instantaneous process. In the Sec.5 we will study some characteristics of flux pulses produced by avalanches in our model.

This paper is organised as follows: in the Sec. 2 the one-dimensional transport model is introduced. The Sec. 3 is dedicated to investigation of dependency between gradients and fluxes. The Sec. 4 deals with the studies of transport correlations. Flux pulse are considered in the Sec. 5. Finally, comments and conclusions are discussed in the Sec. 6.

## 2. Model description

The transport of the averaged density  $h(x)$  is driven by the root-mean-square fluctuations  $\phi(x)$  as follows

$$\frac{\partial h}{\partial t} = \frac{\partial}{\partial x} \left( \mu_0 \phi \frac{\partial h}{\partial x} \right) + S_0, \quad (1)$$

$$\frac{\partial \phi}{\partial t} = \phi (\gamma - \mu \phi) + S_1. \quad (2)$$

The Eq. 1 is a transport equation containing the radial diffusion term and the source term  $S_0$ . Here the diffusivity is proportional to  $\mu_0 \phi$  where  $\phi$  are the fluctuations driven by the Eq. 2 and  $\mu_0$  is a constant term to regulate the diffusivity. The latter is called the evolution equation. It contains a linear term responsible for the linear triggering of the instability with growth rate  $\gamma$ , a nonlinear term with a coefficient  $\mu$ , which brings the fluctuations to the saturation level and a source  $S_1$ , which guarantees a minimum level of fluctuations in the numerical simulations. The coefficient  $\gamma$  is proportional to the critical gradient of the instability:

$$\gamma = \gamma_0 \left( -\frac{\partial h}{\partial x} - z_c \right) \Theta \left( -\frac{\partial h}{\partial x} - z_c \right).$$

Here  $z_c$  is the value of the critical gradient and  $\Theta$  is the Heaviside step function. Therefore, if the gradient  $Z = -\partial h/\partial x$  is lower than the critical gradient then the linear growth  $\gamma$  is equal to zero and the fluctuations decrease. In the same way, if the gradient is higher than  $z_c$ , it triggers the fluctuations and therefore the radial diffusion in the Eq. 1 increases.

This transport model is an analogy of the classical running sandpile. The linear term in the Eq. 2 proportional to  $\gamma$  plays the role of the *threshold* in the sandpile, the ratio of coefficients  $\mu/\mu_0$  regulates the *drive* of the system and  $S_0$  can be interpreted as the new grains of sand we add to the system.

The equations are numerically advanced as follows. We add a small quantity to the source terms with some probability, that is

$$\phi_i^t \rightarrow \phi_i^t + \bar{\phi}$$

with probability  $p_1$ , and

$$h_i^t \rightarrow h_i^t + \delta$$

with probability  $p_0$ .

The transport equation given by the Eq. 1 and the evolution equation given by the Eq. 2 are numerically implemented with using the following time-discretisation scheme:

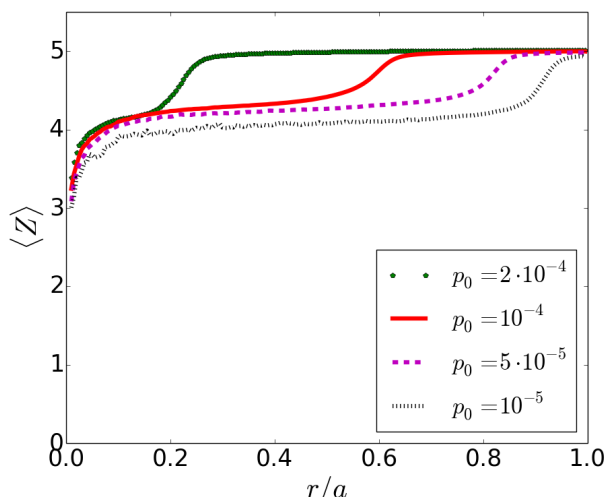


**Figure 1.** The average slope of the profile  $\langle Z \rangle$  is plotted for different values of  $p_0$  (probability to add new grains). Two regions are formed with a clear transition between them. Outer region remains very close to the critical gradient value ( $z = 5$ ) and the inner one at the subcritical state ( $z < 5$ ).  $L=200$ .

$$h_i^{t+\Delta t} = h_i^t + \Delta t \mu_0 \left( -\phi_i^{t+\Delta t} z_i + \phi_{i-1}^{t+\Delta t} z_{i-1} \right),$$

$$\phi_i^{t+\Delta t} = \phi_i^t \exp \left[ \Delta t \left( \gamma_i - \mu \phi_i^t \right) \right],$$

where  $\gamma_i = (z_i - z_c) \Theta(z_i - z_c)$ , with  $z_i = h_i^t - h_{i+1}^t$ .

We are using the Dirichlet boundary condition  $h(L) = 0$  where  $L$  is the size of the system. For all the results included in this paper the parameters of the simulations have the following values:  $z_c = 5$ ,  $\gamma_0 = 1$ ,  $\mu = 200$ ,  $\mu_0 = 100$ ,  $\Delta t = 0.05$ ,  $\bar{\phi} = 10^{-8}$ ,  $p_1 = 10^{-7}$  and  $\delta = 0.05$ .

The numerical results show that the steady state can be reached. We will focus on the slope  $Z$  of the sandpile height  $h$ . On the Fig. 1 the average slope is presented. We observe that the system self organizes in two regions as follows: the inner region remains at the subcritical state ( $z < z_c$ ), which is a characteristic of SOC systems, while at the outer region a critical region ( $z = z_c$ ) is formed.

In the subcritical region, transport is mostly avalanche-like. Furthermore it exhibits a quasiperiodicity [9] similar to the sandpile model with diffusion [10]. In the critical region the transport is quasicontinuous as we will see in the Sec. 4. The transition point (normalized to  $L$ ) between zones is proportional to  $p_0 L^{3/4} (\mu/\mu_0)^{7/8}$  [5]. In the present paper we will only vary the parameter  $p_0$  which represents the probability to add a sand grain inside the sandpile. We will use  $L = 200$  or  $L = 1200$  to highlight some of the characteristics of system.

### 3. Relation between gradient and flux

Let us focus on the gradients  $Z$  and fluxes  $\Gamma = \mu_0 \phi Z$  inside the system. In any diffusive model the flux is proportional to the gradient. When the gradient increases the flux rises as well. On the same way, lower gradients implies lower fluxes. However, in [6], fluxes and gradients were measured at the edge of different magnetically confined fusion devices: not only the proportional behavior has been not observed but also higher fluxes were found for low gradients. Averaged measurements have shown that the gradients below the mean value involve higher fluxes.

Our simple model exhibits a similar behavior as can be seen on the Fig. 2. On the abscissa we put the values of the gradient normalized to its standard deviation  $\sigma$ . The positive values represent steeper than mean value of the gradient and the negative ones: lower than the mean value of the gradient correspondingly. On the ordinate, we put the values of the flux normalized

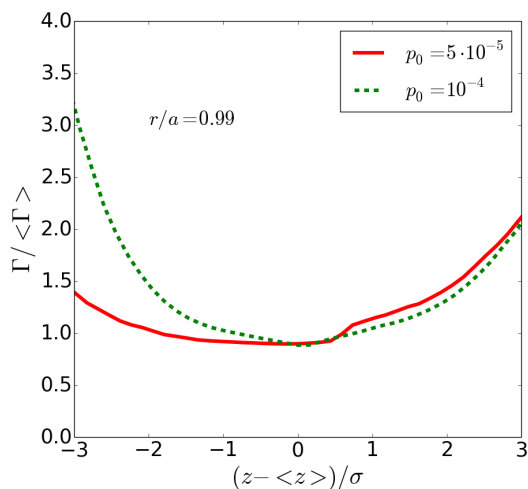


**Figure 2.** The gradient-flux relation for two different values of  $p_0$ . On the abscissa axis: values of gradient normalized to its standard deviation  $\sigma$ . On the ordinate axis: values of flux normalized to its mean value.  $L=200$ .

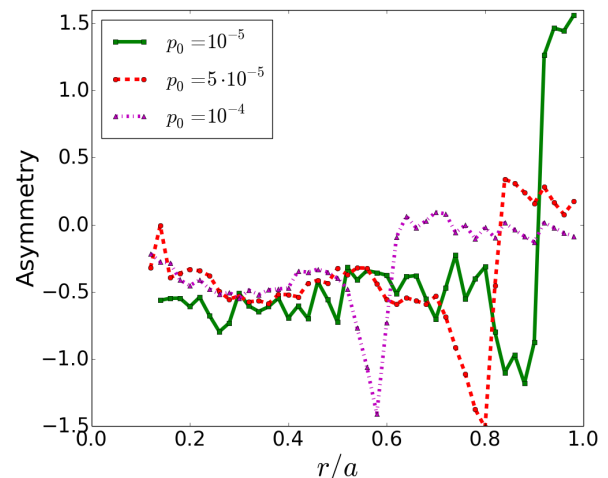


**Figure 3.** The asymmetry function of the gradient-flux relation as a function of position for three different  $p_0$ . Two symmetry regions can be observed for each value of  $p_0$ .  $L=200$

to its mean value. The examples on the Fig. 2 represent measurements at the edge of the system following the experimental setup. The parabolic profile is observed, which supports the idea from the experiments: the system is not following a diffusive transport. This result is observed as well at any other position and for different values of  $p_0$ , which corresponds to a different size of the subcritical region.

Because the gradient-flux relation follows a parabolic profile centered in the most probable gradient, it is interesting to study the symmetry of that profile and how it behaves accordingly to the different parameters of our simulations. We define the asymmetry function as follows:

$$\text{Asymmetry} = \frac{\int \text{flux} \times \text{gradient}}{\int \text{flux}}$$

where fluxes and gradients are normalized following the results on the Fig. 2. The asymmetry function gives us zero if the profile is completely symmetric (a parabola), positive values of the right hand side of the profile presented at the Fig. 2 reaches higher values with respect to its left hand side and the negative ones if inversely, the left hand side of the profile reaches higher values.

The symmetry of the gradient-flux relation for different  $p_0$  is presented on the Fig. 3 as a function of the radial position. A discontinuity is observed in each studied case. This is due to the fact that the position of the measurements reaches the transition between the two regions (subcritical and critical). Furthermore, the symmetry has a dramatic change if the radial position is situated inside the one region or inside the other one. If the radial position where we take a measurement belongs to the subcritical region then the asymmetry will be negative. However, for positions situated in the critical region the asymmetry is close to zero or positive. In addition, for positions close to the edge the asymmetry increases as  $p_0$  decreases (the latter leads to the growth of the subcritical region).

However, the value of zero asymmetry for cases of a large critical region does not mean that the gradient-flux relation is giving always a perfect parabola. In fact, for  $p_0 > 5 \cdot 10^4$  the flux is practically constant and the profile is no longer a parabola but a flat straight line.

Notice, that this simple one-dimensional transport model reproduces the transport behavior observed experimentally [6]. The physical properties of our model are similar to the sandpile: transport is driven through avalanches. We suggest to refer the parabolic behavior of the gradient-flux relation as a non-local transport effect. We suppose that this is due to the fact that the avalanches at close positions can trigger fluxes. For example, a steep gradient situated in an inner position generates a high flux (mass movement), which can be measured at outer positions even with low gradients.

#### 4. Correlations studies. The $R/S$ analysis

In SOC systems, avalanches are produced by the history of the profile, which characterises the dynamical system. In other words, it means that the presence of avalanches is strongly related to presence of memory and correlation [11]. We have studied the correlations in the flux  $\Gamma$  through the  $R/S$  analysis [7] and the calculation of the Hurst exponent [8]. From a time series  $x = \{x_1, x_2, \dots, x_n\}$  of  $n$  values, then the rescaled range  $R/S$  is defined as:

$$\frac{R(n)}{S(n)} = \frac{\max(0, W_1, W_2, \dots, W_n) - \min(0, W_1, W_2, \dots, W_n)}{S(n)},$$

where  $W_k = x_1 + x_2 + \dots + x_k - k\bar{x}$ ,  $\bar{x}$  is the average value of time series and  $S$  is the standard deviation. If the signal is self-similar, then  $R(n)/S(n) \sim n^H$ , where  $H$  is the Hurst exponent. A value  $H = 0.5$  indicates a random series. For values higher than 0.5 the data exhibits correlation and memory. However, values lower than 0.5 illustrate anti-correlation. In a SOC system the Hurst exponent is close to  $H \sim 0.8$  [11].

On the Fig. 4 and the Fig. 5 the results of the  $R/S$  analysis for the flux at the different positions inside the critical and the subcritical regions are respectively shown. We observe that there are two common domains, we call them  $A$  and  $C$ , on both figures.

The domain  $A$  exhibits a Hurst exponent close to the value of 1, which means the presence in the system of a strong correlation. The width of the domains  $A$  gives us an estimation of the correlation time. The latter can be modified if the ratio between sizes of critical/subcritical regions changes: wider subcritical region corresponds to longer correlation time and wider  $A$  domain. The strong correlation of the dynamics comes from the fact that once the avalanche is started, it is most probable that the avalanche continues on the next time step.

Another common domain is the domain  $C$ . The presence of the anti-correlated exponent can be explained due to the finite size of our model. The following behavior is observed for a very long period of time. At some moment all the cells (space discretization) are close to the critical value and a huge avalanche takes place, which moves the system far below the critical point and for some time no avalanche takes place until the system is filled again with new grains. Furthermore, we have observed how the edge between the domain  $C$  and the previous one moves in function of the system size variation. The domain  $A$  and  $C$  have been also observed in SOC systems [11].

The domain  $B$  is specific for the subcritical zone on the Fig. 4. For stationary, non-periodical data the  $H$  exponent varies from 0 to 1. We have measured a higher value preceded by a value close to zero because the system has quasi-periodicities. Peaks are found in the power spectra (not shown here) that indicates the periodicity of avalanches in the system. Nevertheless, they were observed and discussed in a previous work [9]. That behavior is the same as the observed in the sandpile with diffusion [10]. The size of this domain increases as the system increases because the size of the domain  $C$  decreases.

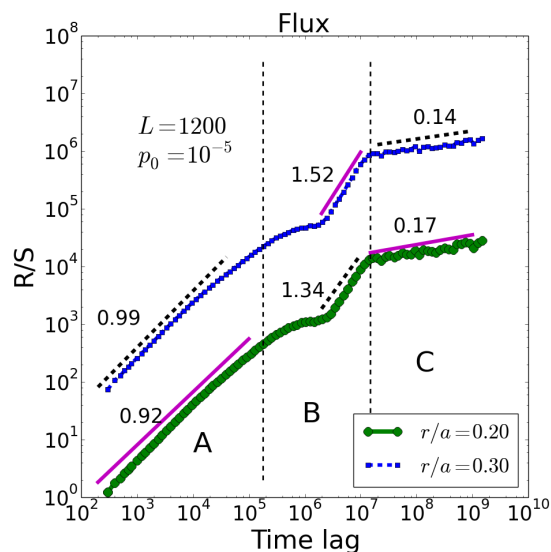


**Figure 4.** The R/S analysis at the subcritical positions. The ordinate axis values have been shifted for convenience. Three domains with different dynamics are observed. The domain *A* demonstrates the correlations of avalanches with themselves. The domain *B* illustrates the quasi-periodicity. The finite size effects belong to the *C* domain.

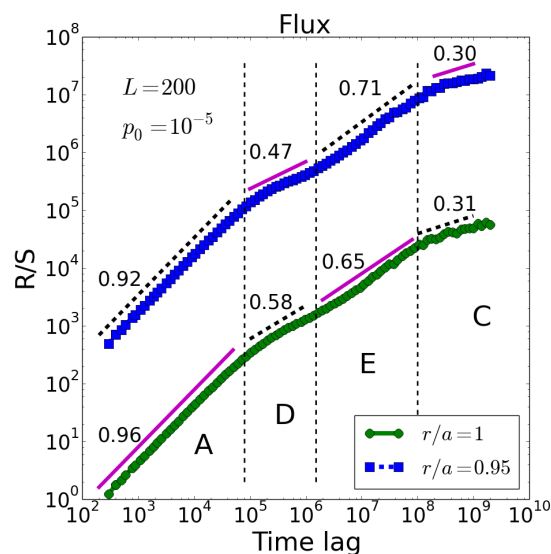


**Figure 5.** The R/S analysis at the critical positions. The ordinate axis values have been shifted for convenience. Two additional domains to the Fig. 4 are observed. The appearance of the domain *D* is due to the proximity to the critical state. The long time correlations are present in the domain *E*.

For the critical region on the Fig. 5, we observe a non correlated or random domain in the domain *D*. The randomness of the  $H \sim 0.5$  is due to the fact that the system is at the critical state ( $z = z_c$ ) at that position. A random  $H \sim 0.5$  is a characteristic of diffusive systems. In addition, for simulations where the critical region is dominant or  $L$  is big enough and the critical region is wider, the *E* domain can disappear and is replaced by the *D* one.

Finally, the *E* domain exhibits correlations at long times for the flux. It is one of the main characteristics of the SOC systems [11], it states that our system has memory for long times. Even at the critical region the model exhibits no diffusive transport and that is why the gradient-flux relation still exhibits the parabola-like profile at the edge. Flux created by the avalanches in the interior can travel to the critical region and modify the transport.

## 5. Flux pulses

In the subcritical region the flux is bursty as demonstrated on the Fig. 6, however at the outer region there is a continuous flux with perturbations, which leads to the long time correlations. The flux data exhibits a sawtooth profile with very fast growths and long tails during the relaxation. Values of flux vary between several orders of magnitude. Remark that the avalanches in the model can propagate inward [5] while fluxes are always positive, pointing outward.

Since the flux in the subcritical region exhibits an intermittent behavior, we will not focus on the instantaneous flux but on the integrated flux (or pulses). We have used two kind of methods to measure the pulses. The first one integrates the flux from a local minimum to the next one. The second method demeans the flux data and then the pulse is defined from a zero value to the next zero value (but only positive ones). Therefore the last method eliminates all the small

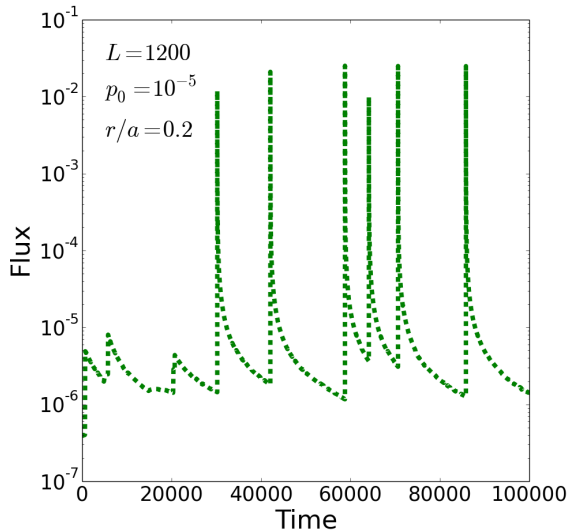


**Figure 6.** Flux at a subcritical position.

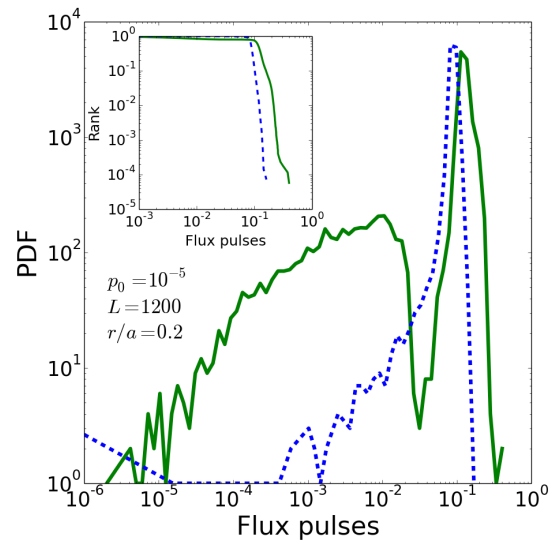


**Figure 7.** The PDF of the pulses (solid line) and the demeaned ones (dashed line). Inset figure: Rank function.

pulses.

The PDF of both methods is presented on the 7. The solid line corresponds to the first method: we can observe a hump and a sharp peak towards local maximum. The second one (dashed line) gives only one global maximum. Therefore we can conclude that the presence of the sharp peak is a consequence of the large pulses because the second method lacks of the small ones.

The peak in the PDF indicates that most of the larger pulses have similar size. In fact, the rank function (inset figure in Fig. 7) reinforces that statement.

Furthermore, we studied the correlations of the flux pulses. On the Fig. 8 the R/S analysis for two different positions at subcritical and critical regions is presented. The subcritical position exhibit three domains. The first domain reveals a correlation among pulses. Then, a higher value of  $H$  is identified, which agree with the quasiperiodicity of the system shown in the domain B. The finite system size effect observed in the domain C are also observed on long times. On the other hand, for positions close to the edge, a correlation is observed again. Then, as the system is larger in this example ( $L = 1200$ ) the domain D dominates and the pulses behave as a diffusive system. Due to the randomness, no system size effect is observed.

## 6. Conclusions

The one-dimensional model based on critical-gradient fluctuations has been used to reproduce the experimental results of the Ref. [6]. The model shows that a simple dynamical system with avalanches exhibits similar transport properties. The avalanches can generate flux in different positions in a way that the relation between gradient and flux exhibits parabola-like profile, which in its turn indicates the non-locality of transport.

In addition, we have studied through the R/S analysis the correlations in the system. Within that analysis, the quasi-periodicities have been identified inside the subcritical region, the similar behavior has also been observed in Ref. [9]. Then, we have measured long time correlations, which have been studied in SOC systems [11]. It indicates that the considered one dimensional transport model has a long time memory.

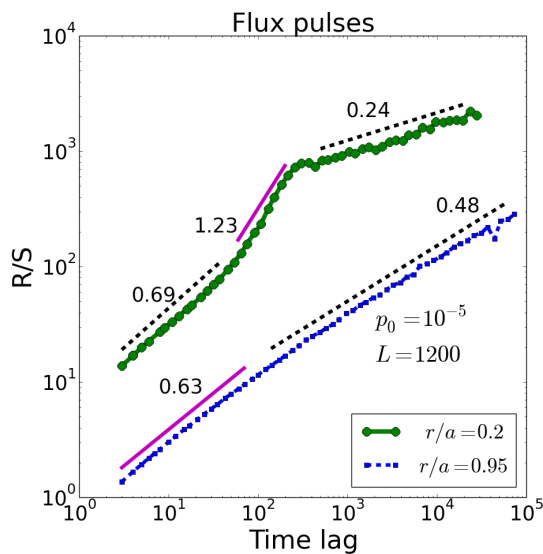


**Figure 8.** The R/S analysis of the flux pulses at positions in the critical and subcritical region. The inner position exhibits the correlation between pulses, then the quasiperiodicity and the anticorrelation due to finite system size. The edge position exhibits the low correlation followed by random behavior.

Finally, we have examined some of the characteristics of the flux pulses in the system. The PDF demonstrates that the majority of pulses are the largest ones and have a similar size. The R/S analysis reveals that the flux pulses are also correlated and the quasiperiodicity of dynamics is present.

## 7. Acknowledgments

Authors gratefully acknowledge very useful discussion with D. Newman and R. Sánchez. This research is sponsored by Ministerio de Economía y Competitividad of Spain under project ENE2012-38620-C02-02 and UNC313-4E-2361. Fruitful interactions with members of the ABIGMAP research network, funded by the Spanish National Project MAT2015-69777-REDT, is also acknowledged.

## 8. References

- [1] Bak P, Tang C and Wiesenfeld K 1987 *Phys. Rev. Lett.* **59** 381-384
- [2] Diamond P H and Hahm T S 1995 *Phys. Plasmas* **2** 3640
- [3] Newman D E, Carreras B A, Diamond P H and Hahm T S 1996 *Phys. Plasmas* **3** 1858
- [4] Sánchez R, Newman D E 2015 *Phys. Control Fusion* **57** 123002
- [5] García L, Carreras B A and Newman D E 2002 *Phys. Plasmas* **9** 841
- [6] Hidalgo C, Silva C, Carreras B.A., van Milligen B Ph, Figueiredo H, Garcia L, Pedrosa M A, Gonçalves B and Alonso A 2012 *Phys. Rev. Lett.* **108** 065001
- [7] Mandelbrot B and Wallis J 1969 *Water Resour. Res.* **5** 967
- [8] Hurst H 1951 *Trans. Am. Soc. Civil Eng.* **116** 770-84
- [9] García L and Carreras B A 2005 *Phys. Plasmas* **12** 092305
- [10] Sánchez R Newman D E and Carreras B A 2001 *Nucl. Fusion* **41** 247
- [11] Woodard R, Newman D E, Sánchez R and Carreras B A 2007 *Physica A* **373** 215